

Exploring implication of variation in biochar production on geotechnical properties of soil

Article

Accepted Version

Ganesan, S. P., Bordoloi, S., Ni, J., Sizmur, T. ORCID: <https://orcid.org/0000-0001-9835-7195>, Garg, A. and Sekharan, S. (2020) Exploring implication of variation in biochar production on geotechnical properties of soil. *Biomass Conversion and Biorefinery*. ISSN 2190-6823 doi: <https://doi.org/10.1007/s13399-020-00847-2> Available at <https://centaur.reading.ac.uk/91810/>

It is advisable to refer to the publisher's version if you intend to cite from the work. See [Guidance on citing](#).

To link to this article DOI: <http://dx.doi.org/10.1007/s13399-020-00847-2>

Publisher: Springer

All outputs in CentAUR are protected by Intellectual Property Rights law, including copyright law. Copyright and IPR is retained by the creators or other copyright holders. Terms and conditions for use of this material are defined in the [End User Agreement](#).

www.reading.ac.uk/centaur

CentAUR

Central Archive at the University of Reading

Reading's research outputs online

1 **Exploring implication of variation in biochar production on geotechnical properties of soil**

2
3 Suriya Prakash Ganesan, Sanandam Bordoloi, Junjun Ni*, Tom Sizmur, Ankit Garg*, Sreedeeep Sekharan

4
5 **Name:** Suriya Prakash Ganesan

6 **Title:** Master's student

7 **Affiliation:** Institute of Civil Engineering, Qingdao University of Technology, China

8 Department of Civil and Environmental Engineering, Shantou University, China

9 **Address:** Institute of Civil Engineering, Qingdao University of Technology, China

10 **E-mail:** suriyaganesan1075@gmail.com

11
12 **Name:** Sanandam Bordoloi

13 **Title:** Post-Doctoral fellow

14 **Affiliation:** Department of Civil and Environmental Engineering, Hong Kong University of Science and
15 Technology, China

16 **Address:** Department of Civil and Environmental Engineering, Hong Kong University of Science and
17 Technology, China

18 **E-mail:** sanandam@ust.hk

19
20 **Name:** Dr Junjun Ni* (Corresponding author)

21 **Title:** Visiting Assistant Professor

22 **Affiliation:** Department of Civil and Environmental Engineering, Hong Kong University of Science and
23 Technology, China

24 **Address:** Department of Civil and Environmental Engineering, Hong Kong University of Science and
25 Technology, China

26 **E-mail:** cenijj@ust.hk

27
28 **Name:** Dr Tom Sizmur

29 **Title:** Associate Professor

30 **Affiliation:** Department of Geography and Environmental Science, University of Reading, United
31 Kingdom

32 **Address:** Department of Geography and Environmental Science, University of Reading, United Kingdom

33 **E-mail:** t.sizmur@reading.ac.uk

34
35 **Name:** Dr Ankit Garg* (corresponding author)

36 **Title:** Associate Professor

37 **Affiliation:** Department of Civil and Environmental Engineering, Shantou University, China

38 **Address:** Department of Civil and Environmental Engineering, Shantou University, China

39 **E-mail:** ankit@stu.edu.cn

40
41 **Name:** Dr. Sreedeeep S

42 **Title:** Professor

43 **Affiliation:** Department of Civil Engineering, Indian Institute of Technology Guwahati, India.

44 **Address:** Department of Civil Engineering, Indian Institute of Technology Guwahati, India

45 **E-mail:** srees@iitg.ac.in

50 **Abstract**

51 Biochar produced from the pyrolysis of plant based feedstock has been advocated as an alternative
52 soil amendment for landfill cover. Previous literature indicated that the pyrolysis temperature
53 influences the intra-pore distribution and surface functional groups (especially hydroxyl groups),
54 resulting in “love-hate relationship” of the biochar amended soil (BAS) with water. From the
55 purview of geotechnical engineering, the effect of pyrolysis temperature on geotechnical
56 properties are rarely investigated. In total, three biochar rates (0, 5 and 10%) were considered for
57 a set of geotechnical experiments in sand clay mixture soil with biochar produced at 350 °C and
58 550 °C. Test results show that biochar addition in soil, in general regardless of pyrolysis
59 temperature, increased the optimum moisture content (OMC), plasticity index, soil water retention
60 characteristics (SWRC) and decreased the maximum dry density (MDD), shear strength
61 parameters (cohesion, friction), erosion rates. Whilst comparing the pyrolysis temperature effects
62 on two biochar amended soils, only marginal effects (in terms of magnitude) on SWRC were
63 observed. The most significant decrease of MDD (or increase of OMC) for 5% (w/w) and 10%
64 (w/w) biochar additions occurred at pyrolysis temperatures of 550 °C and 350 °C, respectively. In
65 addition, biochar produced at lower pyrolysis temperature (350 °C) was more effective in reducing
66 cracks and enhancing shrinkage area ratio. 10% biochar addition with pyrolysis temperature of
67 350 °C was the optimum combination in resisting soil erosion. The study provides evidence that
68 the geotechnical properties of biochar amended soils for landfill cover soil applications could be
69 tailor made by controlling the pyrolysis temperature.

70 **Keywords:** cedar wood biochar, hydro-mechanical properties, landfill liner applications, pyrolysis
71 temperature

72
73 **Notation**

74	CW	Cedar Wood
75	BAS	Biochar Amended Soil
76	OMC	Optimum Moisture Content
77	MDD	Maximum Dry Density
78	CIF	Crack Intensity Factor
79	SAR	Shrinkage Area Ratio
80	SWRC	Soil Water Retention Curve

81
82
83
84
85
86
87
88
89
90
91
92
93
94
95
96
97
98
99
100
101
102
103
104
105
106
107
108
109

Statement of Novelty

In this paper, biochars (pyrolyzed from cedar wood feedstock) produced from two different pyrolysis temperatures were amended with soil and examined for geotechnical properties in landfill applications. The previous studies although reported the biochar material impact on soil properties, the influence of pyrolysis temperature in the context of geotechnical assessment has been rarely investigated. This study emphasizes the effect of pyrolysis temperature on various geotechnical properties to better understand the effective utilization of biochar in landfill applications

110

111 **Introduction**

112 Bio-based soil amendment materials have gained traction in the past decade [1, 2]. Among these
113 bio-based amendments, biochar has been rediscovered as a sustainable soil amendment material
114 [3, 4]. Biochar is a carbonaceous porous material obtained from thermal degradation of plant-based
115 lignocellulose material under limited supply of oxygen and elevated temperatures termed as
116 pyrolysis [5, 6]. The conversion of waste ligno-cellulose material into biochar helps in carbon
117 sequestration and has been extensively used in agricultural practices [7]. Recently, soil amended
118 with biochar was advocated as a promising final landfill cover material, as it suitably alters the
119 physical [8, 9], hydraulic [10, 11], mechanical [12, 13] and biological [14] properties of the soil.
120 Biochar addition in soil was found to alter the physical properties such as porosity, saturated
121 hydraulic conductivity, surface area, crack potential and soil water retention characteristics
122 (SWRC) [15-17]. Those changes in soil physical properties may promote the growth of vegetation,
123 which affects the soil hydrological responses and stability of earthen infrastructures [18-21]. The
124 soil mechanical properties such as shear strength, erosion potential and liquefaction potential were
125 also reported to be altered by biochar [22, 23]. These variations in geotechnical properties for
126 biochar amended soil (BAS) is majorly attributed to biochar gradation, intra-pores of biochar and
127 surface functional groups.

128 From the purview of geotechnical engineering, the production conditions (e.g. pyrolysis
129 temperature) and its consequent effect on geotechnical properties has rarely been investigated. It
130 is important to understand these relationships because the pyrolysis temperature plays a pivotal
131 role in determining the biochar particle size, its inherent intra-pore distribution and surface
132 functional groups (whether hydrophilic or hydrophobic) [24]. From a material science perspective,
133 the effect of pyrolysis temperatures and feedstock types on chemical, morphological and physical
134 characteristics has been well documented [25-27]. Studies clearly indicated that the feedstock
135 types affect the biochar yield, elemental compositions and other soil properties such as porosity
136 and bulk density [28]. This is due to variation in cellulose, hemicellulose and lignin for different
137 plant-based biomass [29]. In addition, the “love hate relationship” of soil-biochar composite and
138 water is influenced by the variations of surface functional groups and morphology at different
139 pyrolysis temperatures. In biochar, where a broad spectrum of hydroxyl group (-OH) found at the
140 surface of the biochar, determines the hydrophilic nature of the biochar. Previous studies reported

141 that the hydrophilic nature of the biochar increases its affinity towards water [30, 31]. In the
142 contrary, the biochar produced at higher temperature can increase the number of intrapores
143 (mesopores). The increased intrapores have the ability to store water but possess less affinity
144 towards water due to the hydrophobic nature of the biochar (less pronounced hydroxyl band). As
145 functional groups and biochar intra-pores influence the granular arrangement, water retention and
146 strength characteristics of BAS, it is imperative that the geotechnical properties of the composite
147 with biochar produced at different temperatures need to be explored. This exploration will help
148 geotechnical practitioners have a better understanding on the use of biochar which might pave way
149 to a new direction for classification system for biochar, as is the case for fly ash [32].

150 The overarching aim of this work is to provide an elementary understanding of the
151 influence of pyrolysis temperature on the geotechnical properties of BAS. Cedar wood biochar
152 obtained after in-house pyrolysis at 350 °C and 550 °C was mixed with a silty sand soil at 0%, 5%
153 and 10% (w/w). The composites prepared were measured for their compaction characteristics,
154 Atterberg limits, shrinkage and crack area ratio, shear strength, erosion potential and SWRC. The
155 microstructure of biochar and surface functional groups were analyzed beforehand to facilitate the
156 interpretation of these measured parameters.

157

158

159 **Materials and Methods**

160 **Soil and biochar characteristics**

161 An un-amended bare soil and four cedar wood biochar amended soil designated as CW-T-BP (refer
162 Table 1), were analyzed in the current study. The soil was classified as sand clay mixture (SC)
163 according to Unified Soil Classification System [33]. The soil consists of 50% sand (coarse sand-
164 19%, medium sand-16% and fine sand-16%), 19% silt and 30% clay particles. The Atterberg
165 limits, compaction characteristics and specific gravity are tabulated in Table 2. This type of soil
166 has been extensively used as a cover material in landfill liner in countries, such as India, Hong
167 Kong and United States [34-37].

168 The produced biochars were tested for the surface functional groups and significant
169 changes of hydrophilic groups were observed in the biochars pyrolyzed at 350 °C (CW-350) and
170 550 °C (CW-550). CW-350 contained un-pyrolyzed hydrophilic surfaces and functional groups,

171 while CW-550 was fully pyrolyzed and aromatic in nature. These two biochars were selected for
172 further investigation and, since they were broadly representative of low temperature (incomplete)
173 pyrolysis and high temperature (complete) pyrolysis as reported in literature for the selected
174 feedstock [38]. The chemical properties of feedstock and the corresponding biochars are presented
175 summarized in Table 3.

176 **Surface properties of biochar**

177 The morphology of the two produced biochars were analyzed using Field Emission Scanning
178 Electron Microscopy (FE-SEM). Figure 1 clearly showcased the contrasting morphology of the
179 two biochars wherein a high density of intra-pores is observed in case of CW-550. This observation
180 is expected due to the thermal degradation of relatively simple biopolymers (cellulose and
181 hemicellulose), which degrades faster than complex lignin biopolymers [15, 39]. At both
182 magnifications (200X and 1000X), CW-550 reveals a honeycomb intra-pore structure on the
183 entirety of its surface, which was not seen at CW-350. This honeycomb structure is expected as
184 lignin engulfs the cellulose and hemicellulose biopolymers in a similar structural arrangement [40].
185 Figure 2 helps us to understand the surface functional groups of the two produced biochars by
186 analyzing the infrared spectrum of absorption using Fourier Transformation Infra-Red (FTIR)
187 spectroscopy. It is clearly visible that the major hydrophilic functional group i.e. hydroxyl
188 disappears at CW-550 indicated by the apparent reduction of peaks at wavelengths near 3500 cm⁻¹
189 (Fig. 2). In general, the peaks for most of the functional groups are less pronounced for CW-350,
190 compared to CW-550, indicating that the water holding capacity of the biochar would be reduced
191 with higher pyrolysis temperatures.

192 **Experimental setup and procedure**

193 The shrinkage area ratio (SAR) and crack intensity factor (CIF), which gives an indication of the
194 shrinkage and desiccation potential of soil was measured using image analysis [36, 41, 42]. For
195 CIF and SAR experiments, all the soil samples were prepared at liquid limit state in a cylindrical
196 mould (20 cm in diameter) and the samples were allowed to dry naturally at room temperature. At
197 regular interval of 60 minutes, images of the surface area and the corresponding water content in
198 the soil have been monitored. The CIF and SAR values were calculated from the image analysis
199 of the obtained pictures.

200 For erosion assessment, the BAS samples are statically compacted within the mold having
201 the dimensions of 2.5 cm diameter and 5 cm length, respectively. A 7 mm diameter opening is
202 drilled at the center of the sample along the axis. The size of the hole was based on the
203 consideration that the higher flow rates require a bigger hole to initiate erosion and a small hole
204 may cause significant re-deposition of eroded particles on its walls [43]. Drilled samples were
205 installed in pinhole setup and was subjected to different increasing continuous flowrates. The
206 eroded particles were collected by passing the eroded effluent through Whatman filter paper (Fig.
207 5e). The eroded mass was estimated by oven drying method. The shear stress and erosion rate for
208 a specific flow rate was estimated. The corresponding critical shear stress and erodibility
209 coefficient were estimated for every soil state as done previously by Kumar et al. [23]

210 The shear strength parameters such as cohesion and friction angle were measured using the
211 direct shear apparatus. The soil samples were prepared in a shear box of dimension 60 mm*60
212 mm*50 mm at maximum density obtained from the compaction characteristics. The instrument
213 provides the shear stress value for the applied normal stress. The shear strength parameters of
214 cohesion and friction angle were obtained from the shear stress vs normal stress plots. The soil
215 water retention curve was measured using WP4C dew point potentiometer, which gives the
216 indirect measurement of soil suction using the kelvin equation considering the humidity of the air
217 above soil sample [44]. The gravimetric water content of the soil sample is measured followed by
218 the suction measurement. The soil samples were prepared at maximum dry density state. All the
219 experiments were repeated three times at a minimum in order to minimize errors and ascertain the
220 variability.

221

222 **Results and Discussion**

223 **Index properties and compaction state of biochar amended soil**

224 The Atterberg limits (liquid limit, plastic limit and shrinkage limit) for bare soil and BAS are
225 reported in Table 2. There is a significant increase in the liquid limit and plastic limit for BAS at
226 both temperatures (350 °C and 550 °C). This observation is attributed to the higher intra pore
227 spaces (Fig. 1) which facilitate more water to be stored in the soil voids as well as in the intra-pore
228 voids [23]. The plasticity index was also sensitive to the addition of biochar, and was increased at
229 higher application rates and at higher pyrolysis temperatures. Figure 3 shows the compaction

230 curves for bare soil and BAS. The maximum dry density and corresponding optimum moisture
231 content (OMC) for the bare soil were 17 kN/m^3 and 17.2%, respectively. It was seen that after
232 addition of biochar, the dry density decreased to $15.5\text{--}13.1 \text{ kN/m}^3$, while the OMC increased to
233 19.1%-25.2%, depending on the amendment rate and pyrolysis temperature. In 5% biochar
234 addition, the magnitude of MDD decrease and OMC increase was higher at CW-550. This can be
235 explained by very finer particle size of the biochar obtained at 550 °C pyrolysis temperature than
236 that at 350 °C. The finer biochar particles at CW-550 increases the specific surface areas [45] and
237 reduces the specific gravity of the composite to a greater extent than those at CW-350. Hence the
238 MDD value decreased and OMC increased significantly at CW-550 for 5% biochar amendment
239 rate. However, for 10% biochar addition, the characteristics are reversed, such that the magnitude
240 of MDD decrease and OMC increase was higher at CW-350. Since the amendment rate is high,
241 the finer particles of biochar at CW-550 tightly clogged soil voids during compaction. This
242 mechanism can be substantiated by the surface morphology images portrayed in Fig. 1 and
243 previous report by [45]. The tightly packed soil-biochar composite with pore clogging is
244 implausible at CW-350 due to quite coarser nature of biochar obtained at 350 °C pyrolysis
245 temperature. Therefore, MDD decrease and OMC increase was found to be higher at CW-350.
246 Based on the above discussion, it can be concluded that biochar particle size has greater influence
247 on compaction characteristics for smaller biochar amendment rate (e.g., 5%). However, for higher
248 amendment rate (e.g., 10%), the compaction characteristics are mainly dominated by pore clogging
249 of fine particles in the composite.

250 **Shrinkage and desiccation potential of biochar amended soil**

251 Figure 4 shows the CIF and SAR variation at different water content for bare soil and BAS. CIF
252 is the ratio of the cracked area at the soil surface to the total area of the soil specimen [42, 46]. As
253 water content decreases, the CIF increases from zero up to a certain value and then levels off
254 indicating peak CIF [36, 47]. The peak CIF decreases with respect to bare soil by almost 73% for
255 both CW-350-5% and CW-350-10%. For CW-550-5% and CW-550-10%, the peak CIF decreases
256 up to 56% and 66%, respectively. At CW-350, as the hydroxyl groups are abundant (seen in the
257 FTIR spectra) and the water present in the resulting BAS naturally results in less cracks. On the
258 other hand, the lesser abundance of hydroxyl groups on the surface of CW-550 means that it retains
259 less water and thus has a higher CIF at both amendment rates compared to CW-350. The SAR
260 indicates the ratio of shranked area to the initial cross-sectional area of soil [48] The BS shrinks to

261 74% of original area whereas CW-350-5% and CW-350-10% shrinks to 86% to 89% of original
262 area relatively at the end of drying. The CW-550-5% and CW-550-10% shrinks up to 75% to 79%
263 of original area, thus showing that CW-350 has better shrinkage mitigation overall (similar to CIF
264 response).

265 **Shear strength and erodibility parameters of biochar amended soil**

266 Figure 5 presents the shear stress versus normal stress response for all soil samples and their
267 respective shear parameters (cohesion (c) and angle of friction (ϕ)). It can be seen that cohesion of
268 BAS decreases with respect to bare soil. The ϕ increases with addition of biochar for both BAS
269 prepared at 350 °C and 550 °C. In the context of amendment rates, for the BAS, the composite
270 prepared at 550 °C showed less cohesion with respect to 350 °C which can be explained by the
271 absence of hydrophilic (-OH) groups. At 350 °C, with an increase in biochar amendment rate, the
272 cohesion increases due to more abundant (-OH) groups. The same is not observed for BAS with
273 CW-550 since cohesion is lower at the higher application rates. At biochar amendment rate 10%,
274 CW-550 has a higher percentage of finer particles than CW-350. The increased fine particles can
275 reduce the contact friction between coarse grains and hence decrease the shear resistance [49].
276 That is why at lower normal stress (50 kPa), CW-550 has much lower shear strength than CW-
277 350. However, with the increase of normal stress to 150 kPa, stress-induced particle rearrangement
278 and clogging of soil pores by finer biochar particles become more significant in CW-550 (Fig. 1).
279 The increase of pore clogging and hence soil density under higher stress in CW-550 causes the
280 interlocking between particles and hence the tendency to soil dilatancy [50], resulting in a higher
281 shear strength.

282 Figure 6 shows the variation of erosion rate with shear stress for bare soil and BAS for
283 three different compaction states (i.e. OMC-5%, OMC and OMC+5%). It was seen that an increase
284 in moisture resulted in decrease in erosion rate for both BS and BAS, which is attributed to
285 apparent cohesive force between soil particles in the presence of water [51] and the particle
286 orientation change from flocculated to dispersed [52]. Runoff water can easily erode the
287 flocculated particles in dry side, as there is edge-to-face interaction. On the other hand, flow
288 happens along the particle surface in dispersed orientation (wet side) producing relatively less drag
289 [53]. The effect of different pyrolysis temperature was evident in the erosion response for BAS
290 constituted by hydrophilic CW-350-5% and CW-350-10%, showing lower erosion with respect to

291 CW-550-5% and CW-550-10%, at all compaction states. Furthermore, the erosion rate decreases
292 with increased amendment rates for both CW-350 and CW-550.

293 **Soil water retention of biochar amended soil**

294 Figure 7 presents the soil water retention response of bare soil and BAS. It was observed that
295 inclusion of both CW-350 and CW-550 in soil increased the water retention capacity of the soil.
296 Regardless of the biochar amendment rate and pyrolysis temperature, all BAS gave a similar SWR
297 response. This response of BAS was also observed by Wong et al. [54] for compacted Kaolinite
298 soil (at 0.9 degree of compaction) amended with peanut-shell biochar (Fig. 7). Thus, it can be
299 inferred that at high suction (beyond 1000 kPa), the effect of different functional groups and intra-
300 pore volume of biochar does not significantly affect the SWR.

301

302 **Conclusions**

303 This study explored the effects of biochar pyrolyzed at 350 °C and 550 °C applied to a silty sand at
304 5% and 10% (w/w) on the geotechnical properties of the amended soil. The microstructure of
305 produced biochar and its surface functional groups revealed that the intra-pores increase, and
306 surface functional group were lower for biochar produced at higher temperature. There is
307 contrasting hydrophobic and hydrophilic characteristics of biochar as pyrolysis temperature
308 increases, due to decrease in -OH groups and higher intra-pore volume, respectively. The pyrolysis
309 temperature played a major role by altering the basic compaction characteristics (increase in OMC
310 and decrease in dry density due to its porous nature) as reported in previous studies. Whilst
311 analyzing the major objective, biochar pyrolyzed at lower temperature (CW-350) mitigates better
312 in cracking and shrinkage potential than the higher temperature residues (CW-550). This is mainly
313 due to the hydrophilic nature of CW-350, which helps at retaining water in the soil-biochar matrix.
314 However, the same advantage contradicts the shear strength properties with decrease in cohesion
315 irrespective of the amendment rates. On the other hand, the soil water retention curves also shows
316 better response when compared with the bare soil, due to the obvious water retention in the
317 intrapores of the biochar. Thus, the biochar produced at lower temperatures might act better in the
318 landfill applications after plant establishment (for strength increase) of the cover surface
319 considering the aspects of energy reduction and cost intensiveness. Besides, the adverse effects of

320 pyrolysis temperature with biochar obtained from different feedstocks and the effect of pyrolysis
321 temperature on leaching potential of BAS should be studied in future.

322

323 **Acknowledgments**

324 The authors would like to acknowledge Shantou University Scientific Research Fund (NTF17007)
325 for the support.

326

327 **References**

- 328 1. Liang S, Han Y, Wei L, McDonald AG (2014) Production and characterization of bio-oil
329 and bio-char from pyrolysis of potato peel wastes. *Biomass Conv Bioref* 5:237-246.
330 <https://doi.org/10.1007/s13399-014-0130-x>
- 331 2. Machineni L (2019) Lignocellulosic biofuel production: review of alternatives. *Biomass*
332 *Conv Bioref*. <https://doi.org/10.1007/s13399-019-00445-x>
- 333 3. Shalini SS, Palanivelu K, Ramachandran A, Raghavan V (2020) Biochar from biomass
334 waste as a renewable carbon material for climate change mitigation in reducing greenhouse
335 gas emissions—a review. *Biomass Conv Bioref* [https://doi.org/10.1007/s13399-020-](https://doi.org/10.1007/s13399-020-00604-5)
336 [00604-5](https://doi.org/10.1007/s13399-020-00604-5)
- 337 4. Singh R, Srivastava P, Singh P, Sharma AK, Singh H, Raghubanshi AS (2019) Impact of
338 rice-husk ash on the soil biophysical and agronomic parameters of wheat crop under a dry
339 tropical ecosystem. *Ecol Indic* 105:505-515. <https://doi.org/10.1016/j.ecolind.2018.04.043>
- 340 5. Liu R, Liu G, Yousaf B, Abbas Q (2018) Operating conditions-induced changes in product
341 yield and characteristics during thermal-conversion of peanut shell to biochar in relation to
342 economic analysis. *J Clean Prod* 193:479-490. [https://doi.org/10.1016/j.jclepro.](https://doi.org/10.1016/j.jclepro.2018.05.034)
343 [2018.05.034](https://doi.org/10.1016/j.jclepro.2018.05.034)
- 344 6. Yang S, Li B, Zheng J, Kankala RK (2018) Biomass-to-Methanol by dual-stage entrained
345 flow gasification: Design and techno-economic analysis based on system modeling. *J*
346 *Clean Prod* 205:364-374. <https://doi.org/10.1016/j.jclepro.2018.09.043>

- 347 7. Jeffery S, Verheijen FG, Van der Velde M, Bastos AC (2011) A quantitative review of the
348 effects of biochar application to soils on crop productivity using meta-analysis. *Agr*
349 *Ecosyst Environ* 144(1):175-187. <https://doi.org/10.1016/j.agee.2011.08.015>
- 350 8. Ulyett J, Sakrabani R, Kibblewhite M, Hann M (2014) Impact of biochar addition on water
351 retention, nitrification and carbon dioxide evolution from two sandy loam soils. *Eur J Soil*
352 *Sci* 65(1):96-104. <https://doi.org/10.1111/ejss.12081>
- 353 9. Abel S, Peters A, Trinks S, Schonsky H, Facklam M, Wessolek G (2013) Impact of biochar
354 and hydrochar addition on water retention and water repellency of sandy soil. *Geoderma*
355 202:183-191. <https://doi.org/10.1016/j.geoderma.2013.03.003>
- 356 10. Wong JTF, Chen Z, Chen X, Ng CWW, Wong MH (2017) Soil-water retention behavior
357 of compacted biochar-amended clay: a novel landfill final cover material. *J Soil Sediment*
358 17(3):590-598. <https://doi.org/10.1007/s11368-016-1401-x>
- 359 11. Yaghoubi P, Reddy KR (2011) Characteristics of biochar-amended soil cover for landfill
360 gas mitigation. In Pan-Am CGS Geotechnical Conference.
- 361 12. Chen XW, Wong JTF, Ng CWW, Wong MH (2016) Feasibility of biochar application on
362 a landfill final cover—a review on balancing ecology and shallow slope stability. *Environ*
363 *Sci Pollut Res* 23(8):7111-7125. <https://doi.org/10.1007/s11356-015-5520-5>
- 364 13. Das O, Sarmah AK, Bhattacharyya D (2016) Bio composites from waste derived biochars:
365 mechanical, thermal, chemical, and morphological properties. *Waste Manag* 49:560-570.
366 <https://doi.org/10.1016/j.wasman.2015.12.007>
- 367 14. Swagathnath G, Rangabhashiyam S, Murugan S, Balasubramanian P (2019) Influence of
368 biochar application on growth of *Oryza sativa* and its associated soil microbial ecology.
369 *Biomass Convers Bioref* 9:341-352. <https://doi.org/10.1007/s13399-018-0365-z>
- 370 15. Pardo GS, Sarmah AK, Orense RP (2018) Mechanism of improvement of biochar on shear
371 strength and liquefaction resistance of sand. *Geotechnique* 69(6):471-480.
372 <https://doi.org/10.1680/jgeot.17.P.040>
- 373 16. Ni JJ, Chen XW, Ng CWW, Guo HW (2018) Effects of biochar on water retention and
374 matric suction of vegetated soil. *Geotech Lett* 8(2):124-129. <https://doi.org/10.1680/jgele.17.00180>
- 375

- 376 17. Ni JJ, Bordoloi S, Shao W, Garg A, Xu G, Sarmah AK (2020) Two-year evaluation of
377 hydraulic properties of biochar-amended vegetated soil for application in landfill cover
378 system. *Sci Total Environ* 712:136486. <https://doi.org/10.1016/j.scitotenv.2019.136486>
- 379 18. Ng CWW, Ni JJ, Leung AK (2019a) Effects of plant growth and spacing on soil
380 hydrological changes: A field study. *Géotechnique*. <https://doi.org/10.1680/jgeot.18.P.207>
- 381 19. Ng CWW, Ni JJ, Leung AK (2019b) *Plant-Soil Slope Interaction*. Taylor & Francis. ISBN
382 978-1-138-19755-8. 8. 206p. 1st Edition: 2 Aug 2019.
- 383 20. Ni JJ, Leung AK, Ng CWW (2019a) Modelling effects of root growth and decay on soil
384 water retention and permeability. *Can Geotech J* 56(7): 1049-1055. [https://doi.org/](https://doi.org/10.1139/cgj-2018-0402)
385 [10.1139/cgj-2018-0402](https://doi.org/10.1139/cgj-2018-0402)
- 386 21. Ni JJ, Leung AK, & Ng CWW (2019b) Unsaturated hydraulic properties of vegetated soil
387 under single and mixed planting conditions. *Géotechnique* 69(6): 554-559. [https://doi.org/](https://doi.org/10.1680/jgeot.17.T.044)
388 [10.1680/jgeot.17.T.044](https://doi.org/10.1680/jgeot.17.T.044)
- 389 22. Reddy KR, Yaghoubi P, Yukselen-Aksoy Y (2015) Effects of biochar amendment on
390 geotechnical properties of landfill cover soil. *Waste Manag. Res* 33(6):524-532.
391 [10.1177/0734242X15580192](https://doi.org/10.1177/0734242X15580192)
- 392 23. Kumar H, Ganesan SP, Bordoloi S, Sreedeeep S, Lin P, Mei G, Garg A, Sarmah AK (2019)
393 Erodibility assessment of compacted biochar amended soil for geo-environmental
394 applications. *Sci Total Environ* 672:698-707. [https://doi.org/10.1016/j.scitotenv.](https://doi.org/10.1016/j.scitotenv.2019.03.417)
395 [2019.03.417](https://doi.org/10.1016/j.scitotenv.2019.03.417)
- 396 24. Liu Z, Dugan B, Masiello CA, Gonnermann HM (2017) Biochar particle size, shape, and
397 porosity act together to influence soil water properties. *PloS One* 12(6):e0179079.
398 <https://doi.org/10.1371/journal.pone.0179079>
- 399 25. Angin D, Şensoz S (2014) Effect of pyrolysis temperature on chemical and surface
400 properties of biochar of rapeseed (*Brassica napus L.*). *Int J Phytoremediat* 16(7-8):684-
401 693. <https://doi.org/10.1080/15226514.2013.856842>
- 402 26. Sun Y, Gao B, Yao Y, Fang J, Zhang M, Zhou Y, Chen H, Yang L (2014) Effects of
403 feedstock type, production method, and pyrolysis temperature on biochar and hydrochar
404 properties. *Chem Eng J* 240:574-578. <https://doi.org/10.1016/j.cej.2013.10.081>

- 405 27. Guizani C, Jeguirim M, Valin S, Limousy L, Salvador S (2017) Biomass chars: The effects
406 of pyrolysis conditions on their morphology, structure, chemical properties and reactivity.
407 *Energies* 10(6):796. <https://doi.org/10.3390/en10060796>
- 408 28. Albuquerque JA, Calero JM, Barrón V, Torrent J, Campillo MC, Gallardo A, Villar R
409 (2014) Effects of biochars produced from different feedstocks on soil properties and
410 sunflower growth. *J Plant Nutr Soil Sci* 177(1):16-25. [https://doi.org/10.1002/
411 jpln.201200652](https://doi.org/10.1002/jpln.201200652)
- 412 29. Bordoloi S, Garg A, Sekharan S (2017) A review of physio-biochemical properties of
413 natural fibers and their application in soil reinforcement. *Adv Civ Eng Mater* 6(1):323-359.
414 <https://doi.org/10.1520/ACEM20160076>
- 415 30. Das O, Sarmah AK (2015) The love–hate relationship of pyrolysis biochar and water: a
416 perspective. *Sci Total Environ* 512:682-685. [https://doi.org/10.1016/j.scitotenv.
417 2015.01.061](https://doi.org/10.1016/j.scitotenv.2015.01.061)
- 418 31. Gray M, Johnson MG, Dragila MI, Kleber M (2014) Water uptake in biochar: The roles of
419 porosity and hydrophobicity. *Biomass Bioenerg* 61:196-205. [https://doi.org/10.1016/
420 j.biombioe.2013.12.010](https://doi.org/10.1016/j.biombioe.2013.12.010)
- 421 32. Roy WR, Thiery RG, Schuller RM, Suloway JJ (1981) Coal fly ash: a review of the
422 literature and proposed classification system with emphasis on environmental impacts.
423 *Environ Geol* 96.
- 424 33. ASTM D2487 (2017) Standard Practice for Classification of Soils for Engineering Purpose
425 (Unified Soil Classification System). ASTM International, West Conshohocken, PA.
- 426 34. Sadasivam BY, Reddy KR (2015) Adsorption and transport of methane in landfill cover
427 soil amended with waste-wood biochars. *J Environ Manag* 158:11-23.
428 <https://doi.org/10.1016/j.jenvman.2015.04.032>
- 429 35. Ng CWW, Chen R, Coo JL, Jian L, Ni JJ, Chen Y, Zhan L, Guo H, Bangwen L (2018) A
430 novel vegetated three-layer landfill cover system using recycled construction wastes
431 without geomembrane. *Can Geotech J* 56(12):1863-1875. [https://doi.org/10.1139/cgj-
432 2017-0728](https://doi.org/10.1139/cgj-2017-0728)
- 433 36. Bordoloi S, Garg A, Sreedeeep S, Lin P, Mei G (2018) Investigation of cracking and water
434 availability of soil-biochar composite synthesized from invasive weed water hyacinth.
435 *Bioresour Technol* 263:665-677. <https://doi.org/10.1016/j.biortech.2018.05.011>

- 436 37. Sheikh J, Bordoloi S, Yamsani S, Sreedeeep S, Rakesh RR, Sarmah AK (2019) Long-term
437 hydraulic performance of landfill cover system in extreme humid region: Field monitoring
438 and numerical approach. *Sci Total Environ* 688:409-423. [https://doi.org/10.1016/
439 j.scitotenv.2019.06.213](https://doi.org/10.1016/j.scitotenv.2019.06.213)
- 440 38. Rodríguez-Vila A, Selwyn-Smith H, Enunwa L, Smail I, Covelo EF, Sizmur T (2018)
441 Predicting Cu and Zn sorption capacity of biochar from feedstock C/N ratio and pyrolysis
442 temperature. *Environ Sci Pollut Res* 25(8):7730-7739. [10.1007/s11356-017-1047-2](https://doi.org/10.1007/s11356-017-1047-2)
- 443 39. Lehmann J, Joseph S (2015) *Biochar for environmental management: science, technology
444 and implementation*. Routledge.
- 445 40. Bordoloi S, Gopal P, Boddu R, Wang Q, Cheng YF, Garg A, Sreedeeep S (2019) Soil-
446 biochar-water interactions: role of biochar from *Eichhornia crassipes* in influencing crack
447 propagation and suction in unsaturated soils. *J Clean Prod* 210:847-859.
448 <https://doi.org/10.1016/j.jclepro.2018.11.051>
- 449 41. Rasband WS (2011) *ImageJ*. US National Institutes of Health, Bethesda, Maryland, USA.
- 450 42. Yesiller N, Miller, CJ, Inci G, Yaldo K (2000) Desiccation and cracking behavior of three
451 compacted landfill liner soils. *Eng Geol* 57(1-2):105-121. [https://doi.org/10.1016/S0013-
452 7952\(00\)00022-3](https://doi.org/10.1016/S0013-
452 7952(00)00022-3)
- 453 43. Reddi LN, In-Mo L, Bonala MVS (2000) Comparison of Internal and Surface Erosion
454 Using Flow Pump Tests on a Sand-Kaolinite Mixture. *Geotech Test J* 23(1):116-122.
455 <https://doi.org/10.1520/GTJ11129J>
- 456 44. Simms P, Soleimani S, Mizani S, Daliri F, Dunmola A, Rozina E, Innocent-Bernard T
457 (2017) Cracking, salinity and evaporation in mesoscale experiments on three types of
458 tailings. *Environ Geotech* 6(1):3-17. <https://doi.org/10.1680/jenge.16.00026>
- 459 45. Liu Z, Dugan B, Masiello CA, Barnes RT, Gallagher ME, Gonnermann H (2016) Impacts
460 of biochar concentration and particle size on hydraulic conductivity and DOC leaching of
461 biochar–sand mixtures. *J Hydrol* 533: 461-472. [https://doi.org/10.1016/
462 j.jhydrol.2015.12.007](https://doi.org/10.1016/
462 j.jhydrol.2015.12.007)
- 463 46. Liu Z, Dugan B, Masiello CA, Gonnermann HM (2017) Biochar particle size, shape, and
464 porosity act together to influence soil water properties. *Plos one* 12(6): e0179079.
465 <https://doi.org/10.1371/journal.pone.0179079>

- 466 47. Li JH, Li L, Chen T, Li DQ (2016) Cracking and vertical preferential flow through landfill
467 clay liners. *Eng Geol* 206:33-41. <https://doi.org/10.1016/j.enggeo.2016.03.006>
- 468 48. Wan Y, Wu C, Xue Q, Hui X (2019) Effects of plastic contamination on water evaporation
469 and desiccation cracking in soil. *Sci Total Environ* 654:576-582.
470 <https://doi.org/10.1016/j.scitotenv.2018.11.123>
- 471 49. Carraro JAH, Prezzi M, Salgado R. (2009) Shear strength and stiffness of sands containing
472 plastic or non-plastic fines. *J Geotech Geoenviron* 135(9): 1167-1178.
473 [https://doi.org/10.1061/\(ASCE\)1090-0241\(2009\)135:9\(1167\)](https://doi.org/10.1061/(ASCE)1090-0241(2009)135:9(1167))
- 474 50. Bolton MD (1986) The strength and dilatancy of sands. *Geotechnique* 36(1): 65-78.
475 <https://doi.org/10.1680/geot.1986.36.1.65>
- 476 51. Chepil WS (1956) Influence of Moisture on Erodibility of Soil by Wind 1. *Soil Sci Soc*
477 *Am J* 20(2):288-292. <https://doi.org/10.2136/sssaj1956.03615995002000020033x>
- 478 52. Lambe TW (1958) The structure of compacted clay. *J Soil Mech Found Div* 84(2):1-34
- 479 53. Grissinger EH (1966) Resistance of selected clay systems to erosion by water. *Water*
480 *Resour Res* 2(1):131-138. <https://doi.org/10.1029/WR002i001p00131>
- 481 54. Wong JTF, Chen Z, Wong AYY, Ng CWW, Wong MH (2018) Effects of biochar on
482 hydraulic conductivity of compacted kaolin clay. *Environ Pollut* 234:468-472.
483 <https://doi.org/10.1016/j.envpol.2017.11.079>
- 484 55. ASTM D422–63 (2007) Standard Test Method for Particle-size Analysis of Soils. ASTM
485 International, West Conshohocken, PA.
- 486 56. ASTM D4318 (2010) Standard Test Methods for Liquid Limit, Plastic Limit and Plasticity
487 Index of Soils. ASTM International, West Conshohocken, PA.
- 488 57. ASTM D1557 (2012) Standard test methods for laboratory compaction characteristics of
489 soil using modified effort. ASTM International, West Conshohocken, PA.
- 490 58. ASTM D854 (2014) Standard Test Methods for Specific Gravity of Soil Solids by Water
491 Pycnometer. ASTM International, West Conshohocken, PA.
- 492 59. ASTM D3080 (2011) Standard test method for direct shear test of soils under consolidated
493 drained conditions. ASTM International, West Conshohocken, PA.

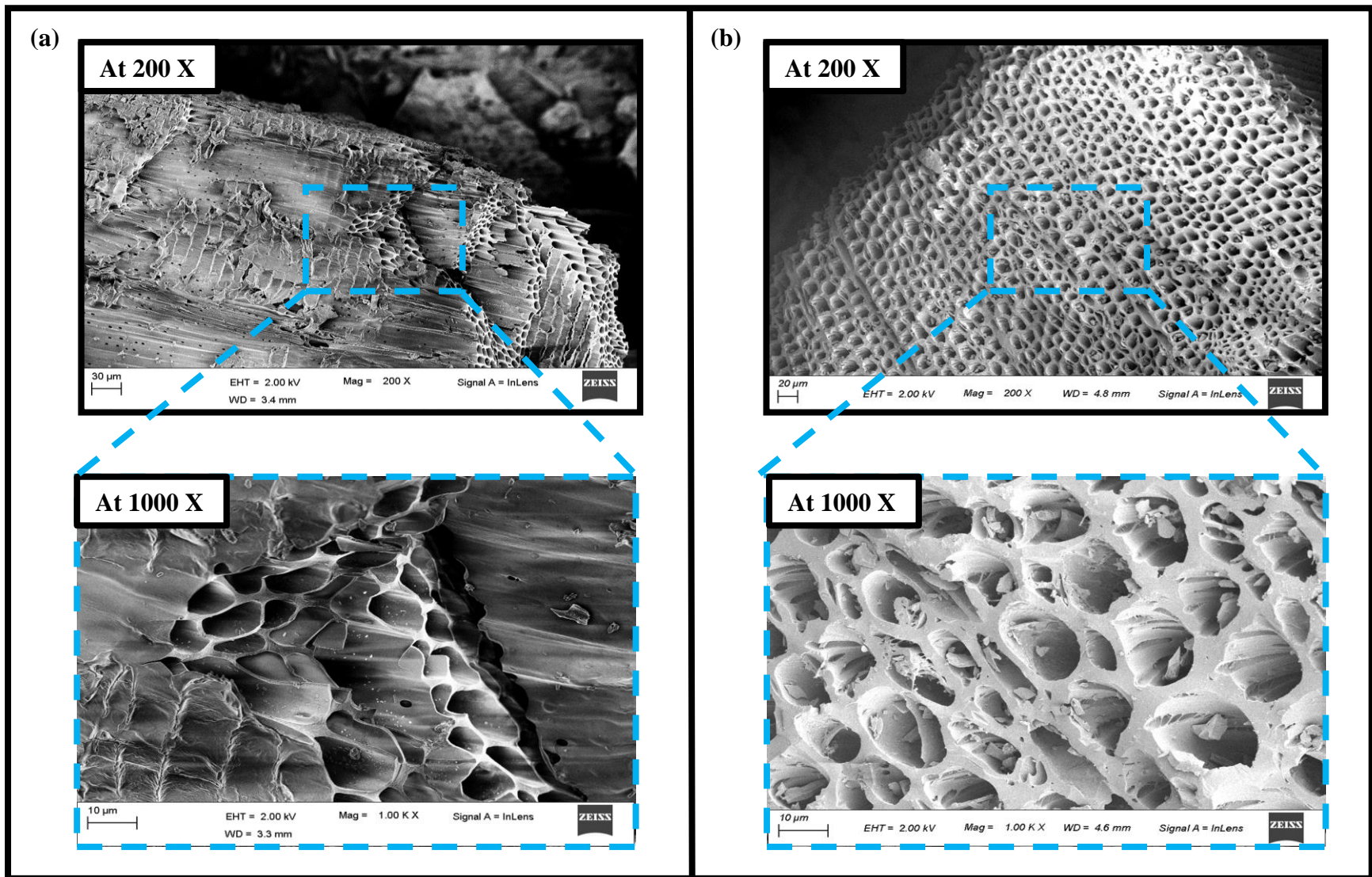


Fig. 1 Surface morphology of cedar wood biochar depicted with FE-SEM images a) 350 °C; b) 550 °C

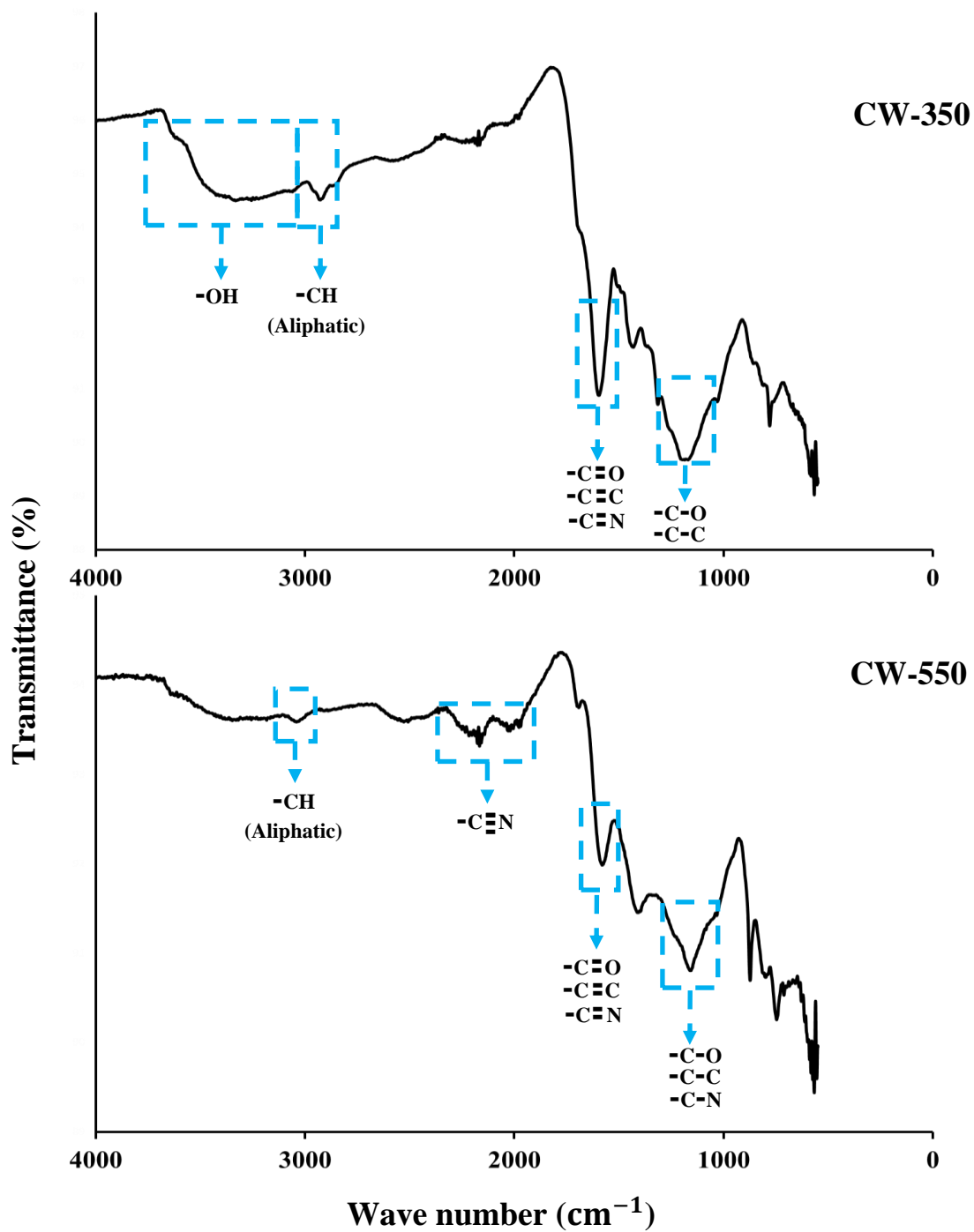


Fig. 2 FTIR results depicting the functional groups of cedar wood biochar at 350 °C and 550 °C

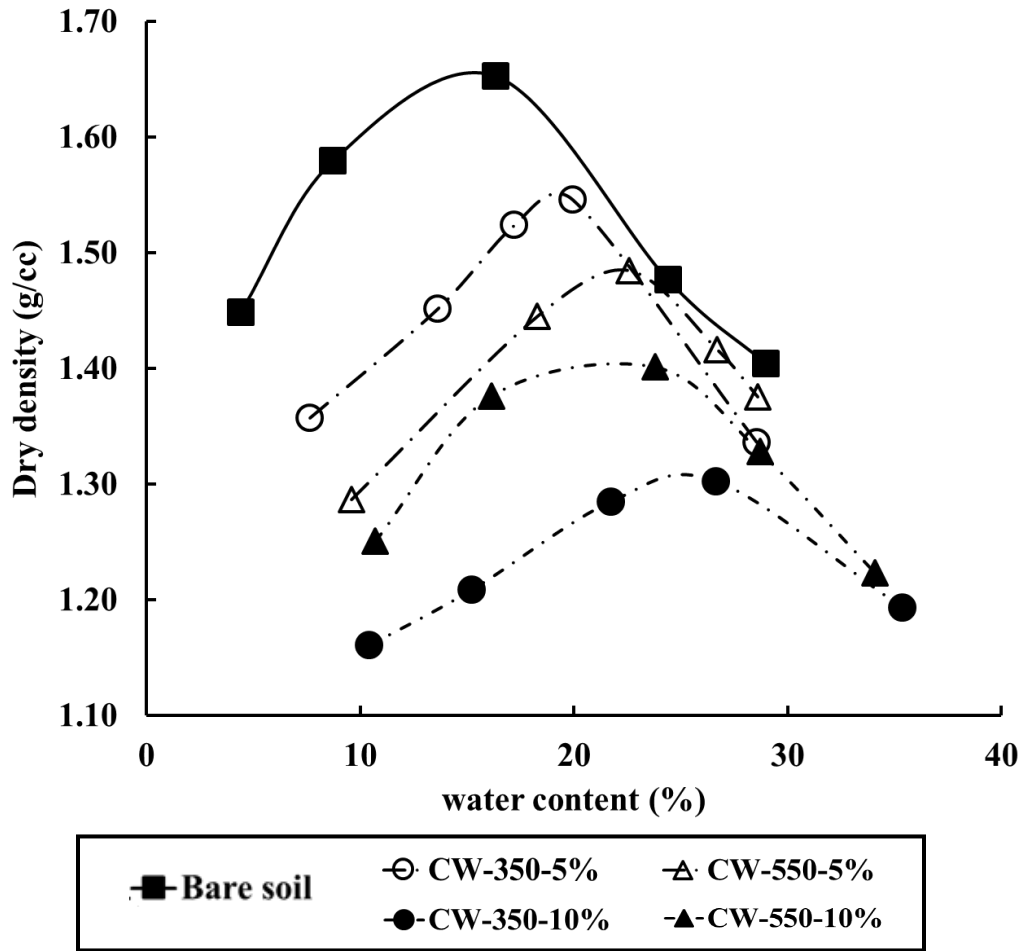


Fig. 3 Compaction curves for bare soil and cedar wood biochar amended soils at 5% and 10%

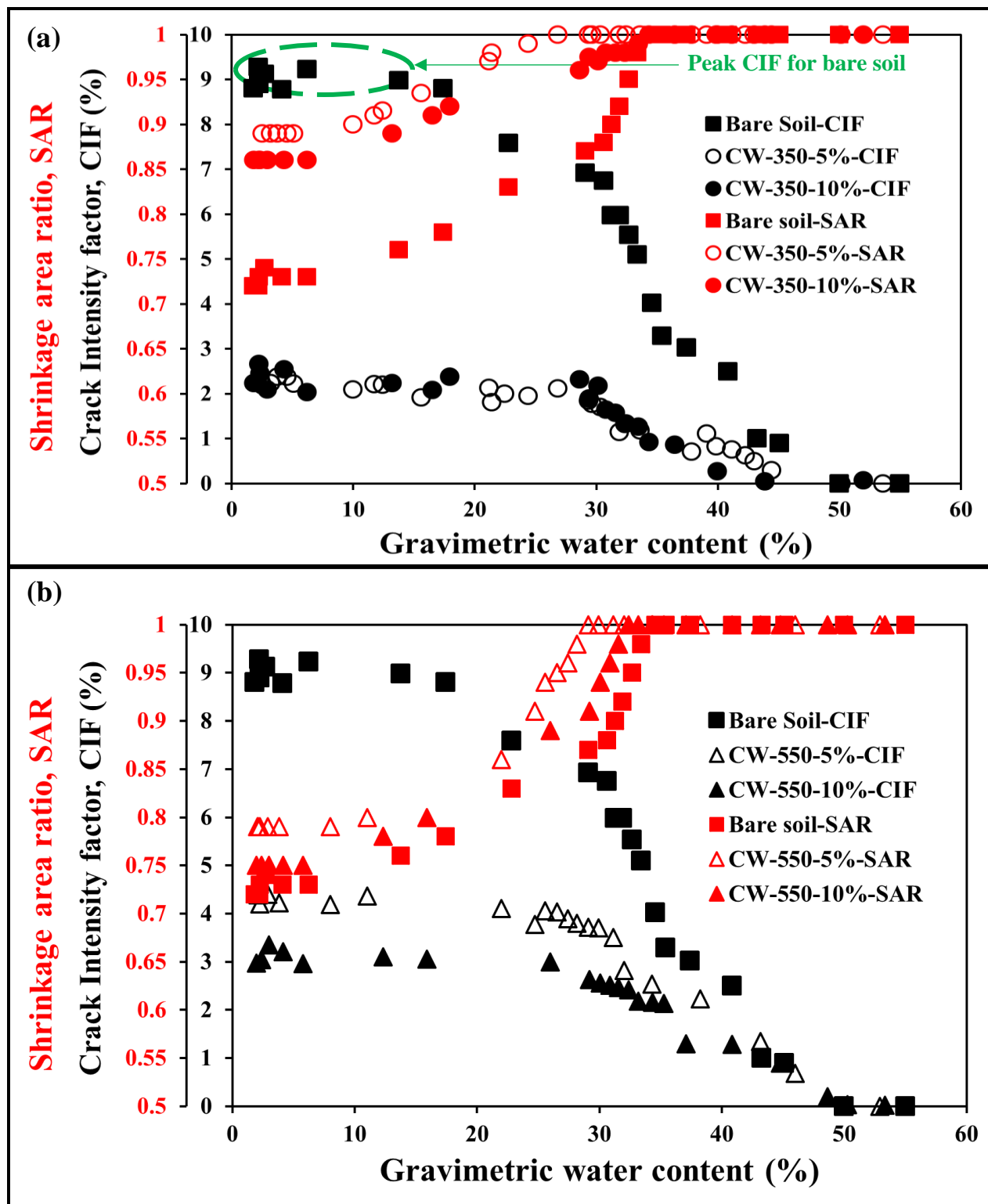


Fig. 4 SAR and CIF variation with moisture content for bare soil and soil-biochar composite produced at (a) 350 °C and (b) 550 °C.

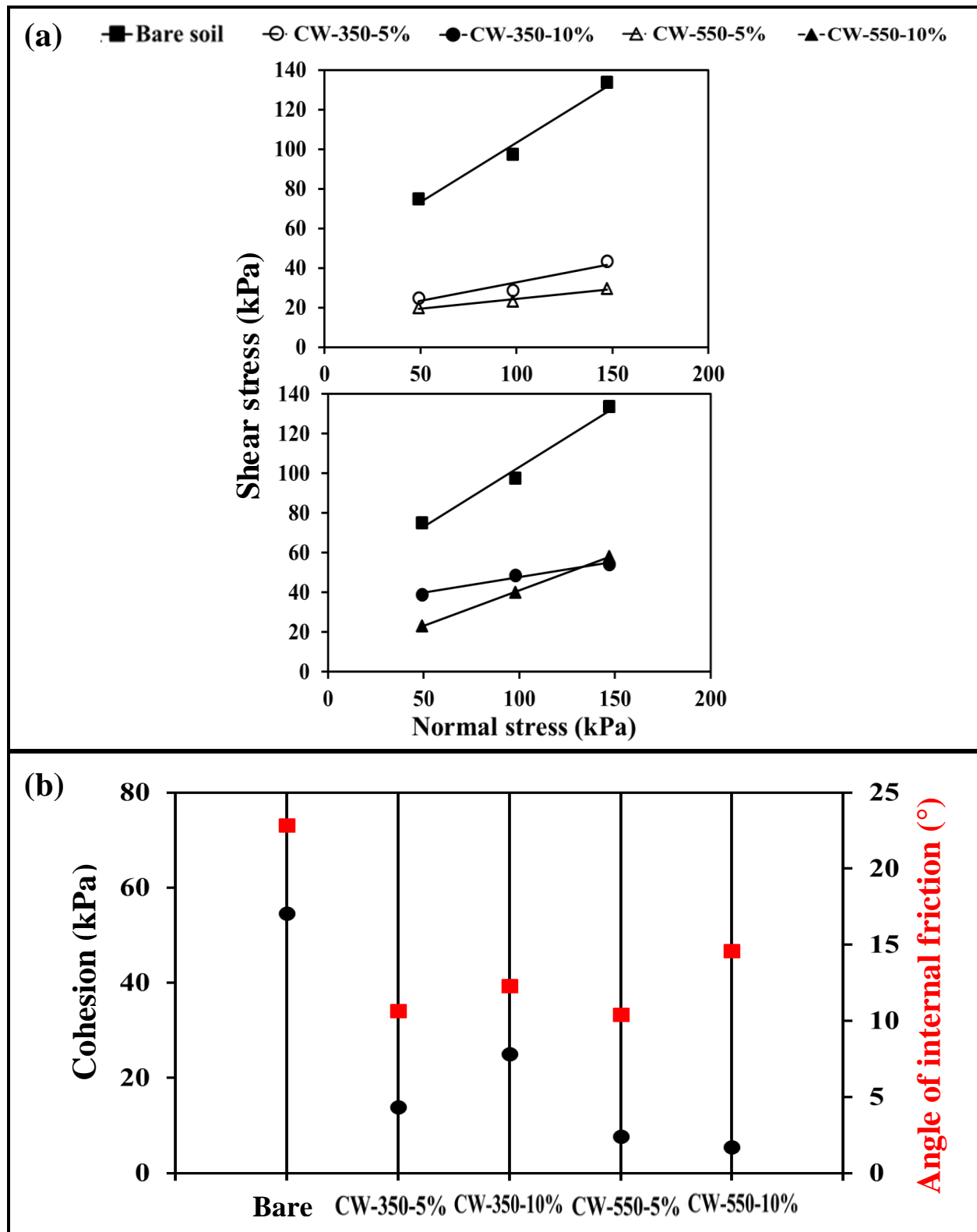


Fig. 5 Direct shear test response for bare soil and biochar amended soil represented as (a) shear stress vs normal stress (b) cohesion and angle of internal friction

Bare soil
 CW-350-5%
 CW-350-10%
 CW-550-5%
 CW-550-10%

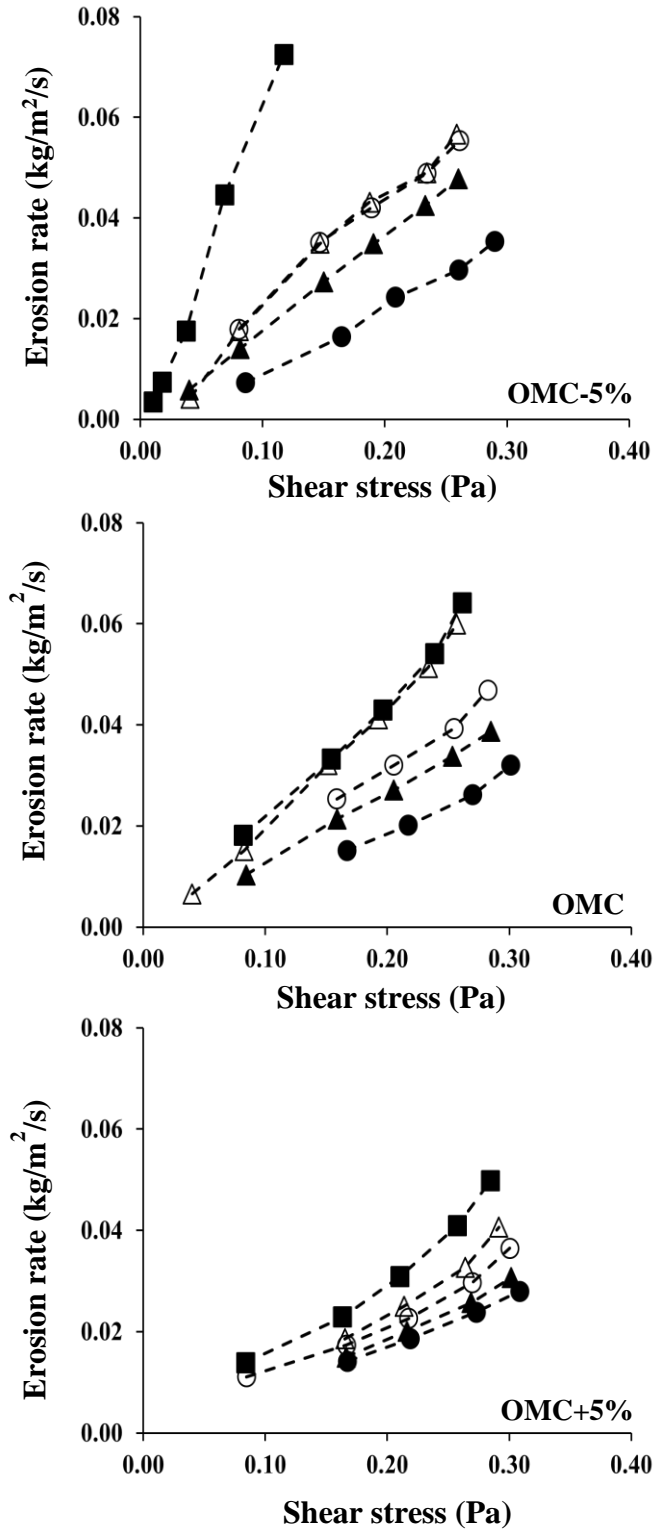


Fig. 6 Pin hole test results representing plots of erosion rate with shear stress

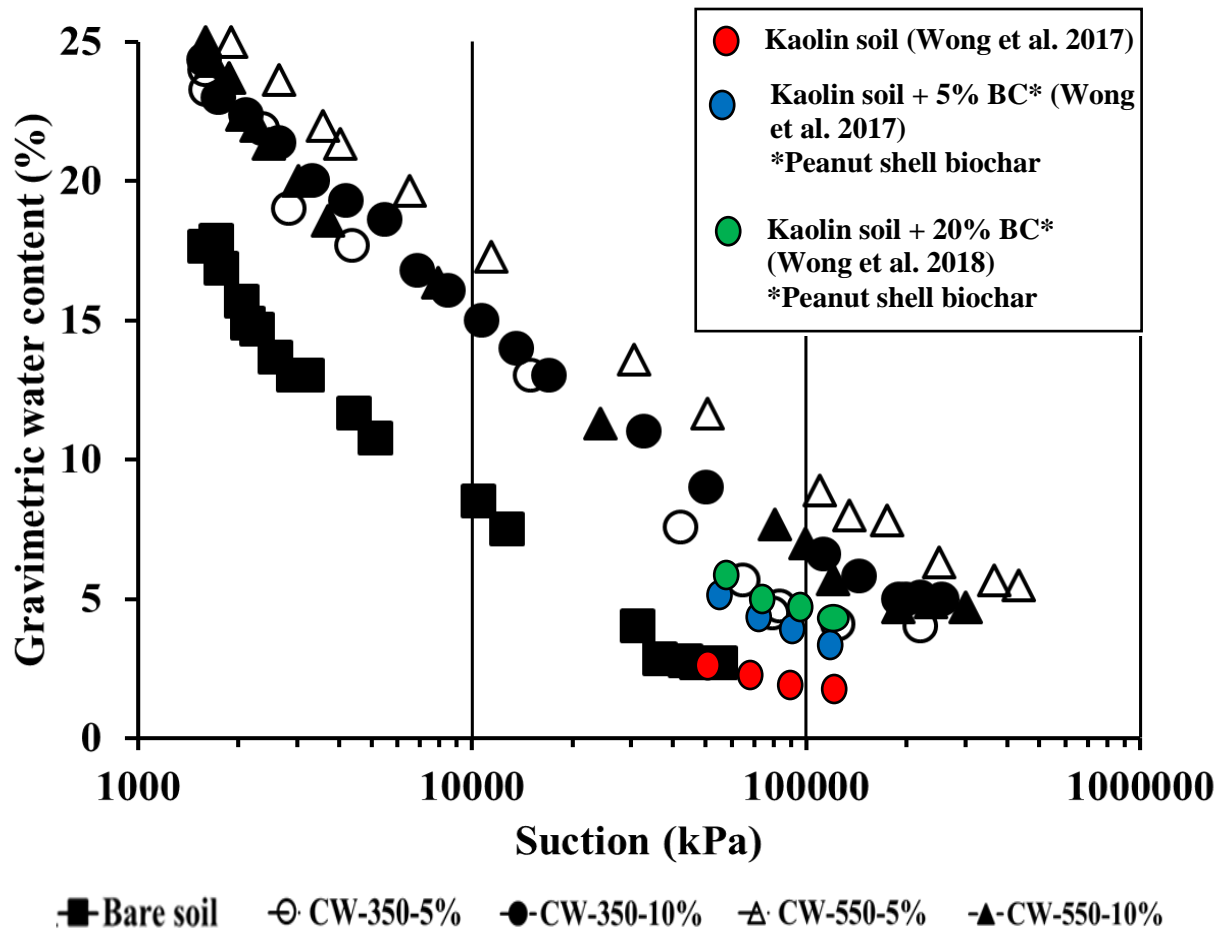


Fig. 7 Soil water retention response for bare soil and biochar amended soil (at 5% and 10%)

Table 1 Designation of materials used to study the geotechnical properties

Test designation	Biochar percentage (%)	Pyrolysis temperature (°C)
BS	NA	NA
CW-350-5%	5	350
CW-350-10%	10	350
CW-550-5%	5	550
CW-550-10%	10	550

Table 2 Physical properties of cedar wood biochar pyrolyzed at 350 °C and 550 °C

Designation	Consistency limits				Compaction parameters		Specific gravity of soil and biochar
	Liquid limit (%)	Plastic limit (%)	Plasticity index	Shrinkage limit (%)	Optimum Moisture Content (%)	Maximum Dry Density (g/cc)	
	ASTM D 4318-00			ASTM D 4943-18	ASTM D 1557-15		ASTM D 854-14
BS	43.6	25.5	18.1	13.9	17.2	1.70	2.74
CW-350-5%	50.4	30.4	20.1	12.7	19.1	1.55	1.11
CW-350-10%	54.4	33.4	21.0	16.4	25.2	1.31	
CW-550-5%	51.9	29.2	22.7	10.2	22.6	1.49	1.08
CW-550-10%	58.5	30.9	27.5	18.4	24.0	1.4	

Table 3 Pyrolysis condition, chemical properties, and particle size of the produced biochar

Feedstock	Cedar wood	
Pyrolysis temperature	350 °C	550 °C
Pyrolysis process	Slow pyrolysis	Slow pyrolysis
Elemental composition		
Carbon (%)	68.71	78.74
Nitrogen (%)	0.41	0.58
Molar ratio		
C: N	168:1	135:1
Ash content (%)	24.1	29.5
CEC (cmol kg⁻¹)	21.67	8.38